2026 IEEE/SICE International Symposium on System Integration (SII)
January 11-14, 2026. Cancún, México

Finger Shape Design based on the Center of Percussion Theory for High-Speed Contact Grasping of Highly-backdrivable Grippers

Yuta Shimizu and Atsushi Kakogawa

***Abstract*— In recent years, grippers that can make high-speed contact and grip objects have been proposed utilizing the high back-drivability of the low reduction ratio geared motors or direct drive motors. However, with simple rotational back-drive phenomena alone, the impact force applied to the rotation axis when the fingertips come into contact with the environment cannot be avoided. Repeated impact forces applying on the actuator could lead to significant damage. Therefore, in this study, the center of percussion (CoP) theory is applied to the finger design of two-fingerd rotational opening-and-closing gripper, which has two highly-backdrivable actuators to independently drive them. This finger shape design theory can lead to the impact force mitigation. In this paper, the impact transmission ratio is considered and the results of experiments that demonstrate the validity and usefulness of the design theory based on the dynamics was presented. The finger design theory was modeled using Newton-Euler equations. As an initial step in the research, the collision experiments at a maximum speed of 1 m/s with a single finger attached to a robot arm were executed. As a result, the proposed CoP-based finger achieved an impact transmission ratio of approximately 0.2, indicating that about 80 % of the impact force was mitigated. Comparisons with other finger shapes further demonstrated the experimental validity and effectiveness of the proposed design.**

I. INTRODUCTION

Pick-and-place operations have been widely recognized as fundamental tasks for industrial robots. In typical industrial robots, due to their heavy and stiff structures, the robotic hand performs grasping without making contact with environmental surfaces such as tables. Additionally, from the perspective of reducing takt time, rapid acceleration and deceleration of the robot motion are required.

However, when geometric information contains errors or when non-contact grasping is difficult, it becomes necessary to take into account physical contact between the end-effector and the environment. To enable high-speed contact grasping, approaches using direct-drive (DD) actuators [1][2] and quasi-direct-drive (QDD) actuators [3]-[5] have been reported. They employ highly backdrivable actuators, leveraging their flexibility and responsiveness (transparency) to mitigate impact forces.

In such applications, flexibility refers to the low constraint force (impedance) against the rotational motion of the drive shaft. Nevertheless, because translational motion of the drive shaft remain constrained, impact forces inevitably arise as constraint forces and cannot be completely avoided. The magnitude of these forces depends on both the impact force acting on the fingertip and the design parameters of the finger. The faster or heavier the fingertip collides, the greater the impact force. In high-speed contact grasping, such repeated impact forces are applied to the drive shaft, which may eventually cause actuator damage or failure [6].

Y. Shimizu and A. Kakogawa are with Department of Robotics, Faculty of Science and Engineering, Ritsumeikan University, 1-1-1 Noji-higashi, Kusatsu, Shiga 525-8577, JAPAN rr0128hi@ed.ritsumei.ac.jp, kakogawa@fc.ritsumei.ac.jp

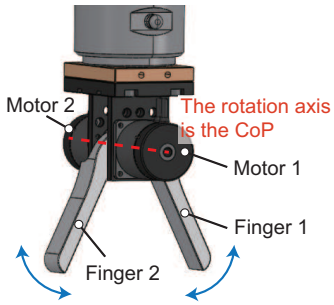

Fig. 1: Conceptual image of the gripper to be developed

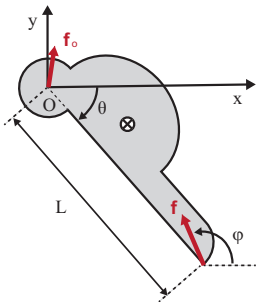

Fig. 2: Dynamic model

This paper describes an approach to minimize the impact force applied to this drive shaft through ingenious finger design. Here, it is assumed that a two-finger independently rotating direct-drive gripper as shown in Fig. 1. Specifically, design conditions based on the center of percussion (CoP) are derived from the Newton-Euler equations (Fig. 2), and their effectiveness is demonstrated through experiments.

The main contributions of this paper are as follows:

- Application of the center of percussion (CoP) theory to an industrial gripper for high-speed contact grasping.
- Finding the design conditions that align the rotational axis with the CoP, whichi is derived from the Newton–Euler equations.
- Experimental validation using a single-finger prototype, assuming a direct-drive, two-finger independently rotating gripper, with collision tests conducted at 1 m/s.

II. CoP THEORY FOR HIGH-SPEED CONTACT GRASPING OF GRIPPERS

To suppress impulsive force during high-speed contact grasping, this study focuses on the concept of the center of percussion (CoP). Here, the CoP refers to the point that remains stationary at the moment of impact when a rigid body undergoes both rotational and translational motions due to an impact force. If this point coincides with the axis of rotation, no impact force is applied translationally while rotated by the impact force.

978-1-6654-5784-2/26/$31.00 ©2026 IEEE

It is important to note that the term CoP has two distinct definitions in the existing literature, which can be highly misleading.

(1) A point that remains stationary at the moment of impact when a rigid body is moved translationally and rotated by an impact force [7]. Alternatively, the impact point where a specific point remains stationary.
(2) The point where the mass should be located when considering the moment of inertia of a rotating rigid body as a concentrated mass [8].

This theory is a well-known classical mechanics principle, and the primary applications in both meanings of (1) and (2) include sports equipment (such as tennis rackets and baseball bats) and tools (such as hammers). For example, gripping a bat at the CoP defined in (1) minimizes impact on the hands, while striking the CoP defined in (2) allows the ball to travel farther.

In this study, we aim to develop a high-speed contact-capable gripper by designing the CoP as defined in (1) to coincide with the rotational center of the finger. Hereafter, in this paper, the term "CoP" refers to the stationary point as defined in (1).

Prior studies have applied the CoP to impact mitigation in various domains: satellite capture by space robots [9], [10], lifting motions in humanoid robots [11], and caster design for wheeled carts [12]. However, to the best of our knowledge, no studies have so far applied the CoP to grippers.

The CoP theory is derived from the impulse of external forces, linear momentum, and angular momentum in a general mechanics textbook [7]. In this paper, to move toward more practical applications, the CoP theory and impact forces are discussed using the Newton-Euler equation and its appropriate assumptions to account for the effects of impact forces near the CoP.

A. Dynamic Model of Gripper Collision

One-degree-of-freedom dynamic model of the gripper is shown in Fig. 2. The rotational axis of the finger is at point O. When a contact force vector $\mathbf{f}$ is applied to the fingertip, a constraint force vector $\mathbf{f}_o$ is generated at the joint (point O). Subsequently, based on the Newton-Euler equation, the following two equations can be formulated by:

$$\mathbf{f} + \mathbf{f}_o = M\ddot{\mathbf{x}}_g \tag{1}$$

$$\mathbf{r}' \times \mathbf{f} + \mathbf{r} \times \mathbf{f}_o = I_g\ddot{\theta}, \tag{2}$$

where M, $\mathbf{x}_g$, $\mathbf{r}'$, $\mathbf{r}$, I_g, and θ denote the mass of the finger and the motor's rotor, the position vector of the center of mass, the position vector from the center of mass to the fingertip, the position vector from the center of mass to the rotational axis, the inertia of the finger and the motor's rotor about its center of mass, and the finger angle in the absolute coordinate system, respectively. Additionally, $\times$ represents the cross product.

In practice, the dynamics are influenced by gravity, the motion of the robotic arm, and rotational viscous resistance. However, since this study assumes high-speed contact in which the external force is sufficiently large, these effects can be neglected. The validity of this assumption will also be demonstrated by the experimental results presented later.

Setting $\theta = 0$ rad as the reference posture, the center of mass position vector $\mathbf{l}_g$ and the fingertip position vector $\mathbf{l}$ can be described as:

$$\mathbf{l}_g = \begin{bmatrix} L_{gx} \\ L_{gy} \end{bmatrix} \tag{3}$$

$$\mathbf{l} = \begin{bmatrix} L \\ 0 \end{bmatrix}, \tag{4}$$

where L_{gx}, L_{gy}, and L denote the distances to the center of mass in x- and y-direction and the length of the finger, respectively. Using the rotational transformation matrix $\mathbf{R}(\theta)$ and the parameters defined above, $\mathbf{x}_g$, $\mathbf{r}'$ and $\mathbf{r}$ can be derived by:

$$\mathbf{x}_g = \mathbf{R}(\theta)\mathbf{l}_g \tag{5}$$

$$\mathbf{r}' = \mathbf{R}(\theta)(\mathbf{l} - \mathbf{l}_g) \tag{6}$$

$$\mathbf{r} = -\mathbf{R}(\theta)\mathbf{l}_g, \tag{7}$$

where

$$\mathbf{R}(\theta) = \begin{bmatrix} \cos\theta & -\sin\theta \\ \sin\theta & \cos\theta \end{bmatrix}. \tag{8}$$

Differentiating (5) twice with respect to time yields the following equation.

$$\ddot{\mathbf{x}}_g = \begin{bmatrix} -(L_{gx}S_\theta + L_{gy}C_\theta)\ddot{\theta} - (L_{gx}C_\theta - L_{gy}S_\theta)\dot{\theta}^2 \\ (L_{gx}C_\theta - L_{gy}S_\theta)\ddot{\theta} - (L_{gx}S_\theta + L_{gy}C_\theta)\dot{\theta}^2 \end{bmatrix}, \tag{9}$$

where S_θ and C_θ mean $\sin\theta$ and $\cos\theta$, respectively. The term of $\dot{\theta}^2$ originates from the centrifugal force. In this study, the gripper collision is assumed to occur against a stationary object surface, such as a table. Therefore, the effect of angular velocity can be neglected while the impact force is applied to the fingertip.

Applying this assumption to (9) and substituting it into (1), it can be rewritten with respect to θ and $\ddot{\theta}$. Similarly, (2) can also be reformulated with respect to θ and $\ddot{\theta}$ by using (6) and (7). Eliminating $\ddot{\theta}$ from these two equations, the relationship among $\mathbf{f}$, $\mathbf{f}_o$, and θ can be obtained. Furthermore, the external force vector $\mathbf{f}$ can be described with its magnitude and the angle ϕ in the absolute coordinate system as follows:

$$\mathbf{f} = \begin{bmatrix} |\mathbf{f}|\cos\phi \\ |\mathbf{f}|\sin\phi \end{bmatrix} \tag{10}$$

An evaluation factor called "impact transmission ratio" is defined as $T(\phi, \theta)$, and it can be obtained by:

$$T(\phi, \theta) = \frac{|\mathbf{f}_o|}{|\mathbf{f}|}. \tag{11}$$

When $T(\phi, \theta) = 0$, the point O coincides with the CoP.

B. Impact Transmission Ratio

Equation (11) represents the ratio of the impact force applied to the joint between the impact force generated at the fingertip, which can be described by:

$$T(\phi,\theta)=\frac{|\mathbf{f}_o|}{|\mathbf{f}|}=\sqrt{\frac{A\sin\{2(\phi-\theta)-\alpha\}+B}{2}}, \tag{12}$$

where

$$A=\sqrt{4Y^2+(X^2-2X+Y^2)^2} \tag{13}$$

$$B=(X^2-1)^2+Y^2+1 \tag{14}$$

$$X=\frac{MLL_{gx}}{I_g+M(L_{gx}^2+L_{gy}^2)} \tag{15}$$

$$Y=\frac{MLL_{gy}}{I_g+M(L_{gx}^2+L_{gy}^2)} \tag{16}$$

$$\alpha=\tan^{-1}\left(\frac{X^2-2X+Y^2}{2Y}\right) \tag{17}$$

Equation (12) results its minimum value of 0 when $A=B$, i.e., $X=1$ and $\sin 2(\phi-\theta)-\alpha=-1$. In other words, at this moment, the impact force generated at the fingertip is not transmitted to the rotational axis, which means force isolation. This phenomenon happens under which the rotational axis coincides with the CoP.

C. Design Conditions for the Gripper

As previously mentioned, the condition for the rotational axis to coincide with the CoP has been derived. However, this condition is not intuitively understandable, making it difficult to design grippers that satisfies it. Therefore, the derived condition is further refined.

1) Condition $X=1$: In (15), the denominator can be considered as the moment of inertia about the rotational axis. Letting it be I_o, X can be described by:

$$X=\frac{MLL_{gx}}{I_o}=1. \tag{18}$$

2) Condition $\sin\{2(\phi-\theta)-\alpha\}=-1$: This condition relates to the angle of the external force applied to the fingertip during contact and the position of the center of mass. Therefore, if there are no restrictions on the finger angle during contact, this condition does not need to be considered during the design process and should instead be taken into account during operation. However, in general, there are often restrictions on the finger contact angle, and thus, it is necessary to consider this condition during the design phase.

If it is assumed that the condition in (18) is satisfied, (16) can be described using X below:

$$Y=\frac{L_{gy}}{L_{gx}}X. \tag{19}$$

Furthermore, L_{gy} and L_{gx} are expressed in the following polar coordinate form.

$$L_{gx}=r_g\cos\theta_g \tag{20}$$

$$L_{gy}=r_g\sin\theta_g, \tag{21}$$

where r_g and θ_g denote the distance to the center of mass and the angular displacement to the center of mass, respectively. Under these equations and the assumption of $X=1$, (19) can be derived by:

$$Y=\frac{\sin\theta_g}{\cos\theta_g} \tag{22}$$

Substituting $X=1$ and $Y=\frac{\sin\theta_g}{\cos\theta_g}$ into (17) and simplifying it, the following equation is obtained:

$$\alpha=2\theta_g-\frac{\pi}{2}. \tag{23}$$

Additionally, the condition $\sin\{2(\phi-\theta)-\alpha\}=-1$ is equivalent to the following:

$$2(\phi-\theta)-\alpha=-\frac{\pi}{2}+2n\pi \quad (n=0,\pm1,\pm2,\dots) \tag{24}$$

Substituting (23) into (24), the following relationship can be yielded:

$$\theta_g+\theta=\phi-\frac{\pi}{2}+n\pi \quad (n=0,\pm1,\pm2,\dots) \tag{25}$$

This means that the external force is perpendicular to the line passing through the rotational axis and the center of mass.

D. Dynamic Effects of the Motor System

In practical applications, the finger is attached to the motor. The rotor and the finger are assumed to be connected as a single rigid body. Then, the total mass of the finger and the motor's rotor M, the center of mass position in the x-direction L_{gx}, and the moment of inertia about the rotational axis I_o can be described as follows:

$$M=M_m+M_l \tag{26}$$

$$L_{gx}=\frac{M_mL_{mgx}+M_lL_{lgx}}{M_m+M_l} \tag{27}$$

$$I_o=I_{mo}+I_{lo}, \tag{28}$$

where M_m, M_l, L_{mgx}, L_{lgx}, I_{mo}, and I_{lo} represents the mass of the rotor, the mass of the finger, the center of mass position of the rotor in the x-direction $(=0)$, the center of mass position of the finger in the x-direction,the rotational moment of inertia of the rotor, the rotational moment of inertia of the finger about the rotational axis, respectively.

Substituting them into the condition (18), it results in

$$X=\frac{M_lLL_{lgx}}{I_{mo}+I_{lo}} \tag{29}$$

Therefore, in condition (18), it is sufficient to consider only the rotational inertia of the motor shaft. Additionally, in condition (25), since the angular displacement of the center of mass θ_g does not change, this condition is not influenced by the parameters of the motor system.

III. EXPERIMENTS

A. Fabricated Finger

As shown in Fig. 3, three types of finger (G1, G2, and G3) were fabricated for the experiment. All of these fingers were made of resin (poly-lactic acid) and fabricated using a 3D printer. In the design of G1, the numerical values in the

(a) G1 (b) G2 (c) G3

Fig. 3: Fingers used for the experiment: (a) finger designed by applying CoP theory to minimize the impact transmission, (b) finger designed with a simple shape, and (c) finger designed to have a high impact transmission ratio for the comparison

TABLE I: Physical parameters of each finger and impact transmission ratio parameters; *when $T(\phi, \theta) = T_{min}$

Parameters	G1	G2	G3
M_l [g]	55.16	31.33	60.39
L [mm]	100	100	100
L_{lgx} [mm]	17.14	44.09	23.16
L_{lgy} [mm]	19.77	5.49	0.15
I_{lo} [g mm^2]	7.87×10^3	9.27×10^3	5.01×10^3
X	1.09	1.37	2.38
T_{min}	0.06	0.37	1.00
$\phi - \theta$ [rad]*	2.47	1.77	0, 3.14

CAD were iteratively applied to the condition in (18) while manually adjusting the design dimensions to maximize θ_g as much as possible. Table I lists the physical parameters, the parameter X from (18) or (29), which determines the impact transmission ratio, the minimum impact transmission ratio T_{min}, and the external force angle $(\phi - \theta)$, was applied to the finger design. Only M_l was measured actually, while the other parameters were calculated in CAD based on the mass M_l. Additionally, for each finger, Fig. 4 plots the impact transmission ratio as a function of the external force angle applied to the finger.

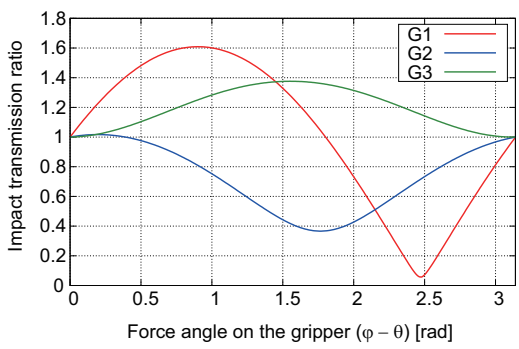

Fig. 4: Simulated results of the external force angle versus the impact transmission ratio among the three types of finger

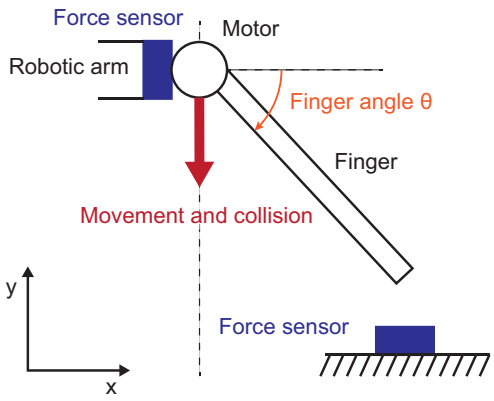

Fig. 5: Schematic diagram of the experiment

B. Experimental Method (Overview)

The outline of the experimental method is illustrated in Fig. 5. A single-finger configuration using a direct-drive motor is installed on a commercialized rigid robotic arm. A force sensor is mounted between the robotic arm and the finger, allowing the measurement of the forces applying to the motor. An another identical sensor is installed on the floor as the collision surface, allowing the measurement of the contact force generated at the fingertip.

The finger angle was kept constant through motor position control, and the end of the robotic arm was moved in the negative y-axis direction to make the fingertip collide. The experiment was conducted with two different robotic arm speeds of 0.5 m/s and 1 m/s. The finger angle θ was varied from 30 deg to 60 deg with the interval of 2 deg and with fifteen trials for each pattern.

C. Experimental System

1) Hardware: The actual experimental system used in this study is shown in Fig. 6. The robotic arm used in this experiment is UR5e (Universal Robots A/S, Denmark). UR5e is equipped with a controller, allowing data transmission and reception via a wired LAN connection to the desktop computer.

The two force sensors used in the experiment are six-axis force sensors, PFS055A251U6 (Leptrino Co., Ltd., Japan). The force rated capacity is 250 N, and 1.2 kHz sampling is possible. Data acquisition is enabled through USB connection to the desktop computer.

A brushless DC motor, MDH(12)-4018-324KE (MICROTECH LABORATORY INC., Japan) was used as an actuator. No reduction gearbox is used, the motor is, however, equipped with an incremental encoder which has a resolution of 1,296,000 Pulse/Rotation (after 4x quadrature). The motor driver MC-200-7200A from the same company was used. The driver allows data transmission and reception via the USB connection to the desktop computer.

2) Software: The robotic arm operation was tested in two experimental conditions, where the arm-end velocity

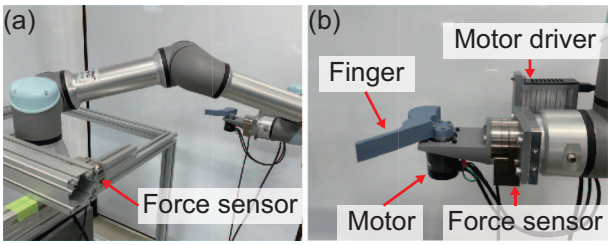

Fig. 6: Experimental System: (a) Overview of the experimental system, (b) The single-finger direct-drive end-effector developed for this study.

at the moment of finger collision was 0.5 m/s and 1 m/s. UR5e allows the input of both velocity and acceleration as command values, and its velocity trajectory follows a trapezoidal profile. The commanded acceleration and motion range were set. Therefore, the finger would collide during the constant velocity phase of the arm-end.

The motor position was controlled to a certain target angle at the moment of collision. Current limit is set to suppress the excessive torque during the collision, which is one of the built-in features of the motor driver MC-200-7200A. For this time, the motor current was limited to 0.5 A. Since the motor's torque constant is 0.071 Nm/A, the output torque of the motor is theoretically limited to approximately 0.036 Nm or less. The value of the current limit was experimentally determined to be the minimum necessary to ensure that the finger angle remained unchanged during the robotic arm's operation. The sampling time of the entire system is 1 ms.

D. Experimental Results

Fig. 7 shows the measurement results of the forces generated at the impact in the collision experiments at 1 m/s. These results were obtained using G1 finger. As the finger angle increases, the force applied at the fingertip becomes larger: approximately 15 N at 30 deg, 20 N at 40 deg, 30 N at 50 deg, and more than 40 N at 60 deg. These results indicate that, in this experiment, at least about 15 N of force was applied to the fingertip, supporting the validity of the assumption used in Section A. Considering that the fingertip force is about 20 times greater than the gravitational force acting on the finger's center of mass (approximately 0.5 N at 1 G), the effects of the gravity and the acceleration can be regarded as negligible compared to the external impact force.

Figure 8 plots the impact transmission ratio obtained from the experiment. $T(\phi - \theta)$ was calculated using (12) and the following equations.

$$|\mathbf{f}_o| = \sqrt{|\hat{F}_{ox}|^2 + |\hat{F}_{oy}|^2} \tag{30}$$

$$|\mathbf{f}| = \sqrt{|\hat{F}_x|^2 + |\hat{F}_y|^2}, \tag{31}$$

where $|\mathbf{f}_o|$ and $|\mathbf{f}|$ denote the magnitudes of the forces applied to the rotational axis and the fingertip, respectively. $|\hat{F}_{ox}|$ and $|\hat{F}_{oy}|$ are the absolute maximum values of the measured force in x- and y-directions obtained from the force sensor

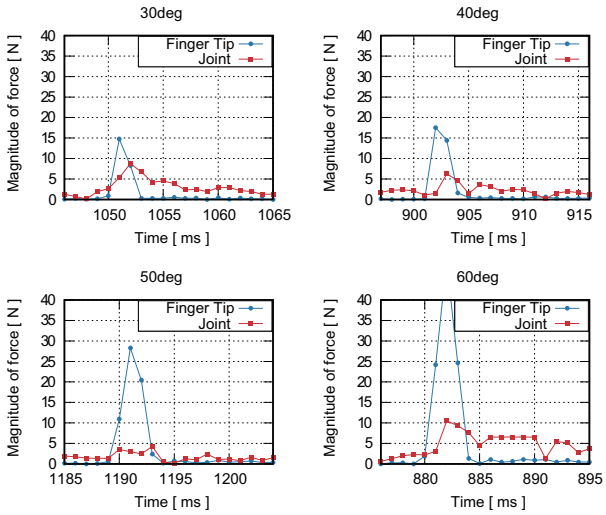

Fig. 7: Measured forces at the moment of impact for finger angles of 30 deg, 40 deg, 50 deg, and 60 deg using G1 finger. The ground-side force sensor represents the force applied to the fingertip, while the robot-arm-side force sensor represents the force transmitted to the actuator.

attached to the robotic arm side, while $|\hat{F}_x|$ and $|\hat{F}_y|$ are those from the force sensor mounted on the floor side. This value is obtained as the peak value within 10 ms from the rise and fall of the force sensor readings. The finger angle θ was obtained from the commanded angle value, and the external force angle ϕ was calculated using the following equation based on the force sensor readings from the floor side.

$$\phi = \tan^{-1} \frac{\hat{F}_y}{\hat{F}_x} \tag{32}$$

IV. DISCUSSION

In the measurement interval, the quadratic approximation of the experimental values showed high correlation with the theoretical values, clarifying that the experiment exhibited the same trend as the theory. A discrepancy in the magnitude and phase can be observed between the theoretical and experimental values, and the primary cause of this is considered to be the filtering effect of the hardware. In this experiment, the force waveforms measured by the force sensor had high frequency of 200-350 Hz, which implies that the electrical filtering effect that the force sensor originally has influenced the results. Furthermore, since the force measured by the force sensor attached to the robotic arm propagates through the finger and motor, the filtering effect is expected to be amplified due to their mechanical impedance. The force sensor attached to the robotic arm may also be affected by the vibrations caused by the movement of the robotic arm.

Although narrowing the gap between the model and the actual system is challenging, the experimental and theoretical values show the same trend, providing evidence that the theory functions correctly. In particular, focusing on the region between 2.5 rad and 2.6 rad, where the impact

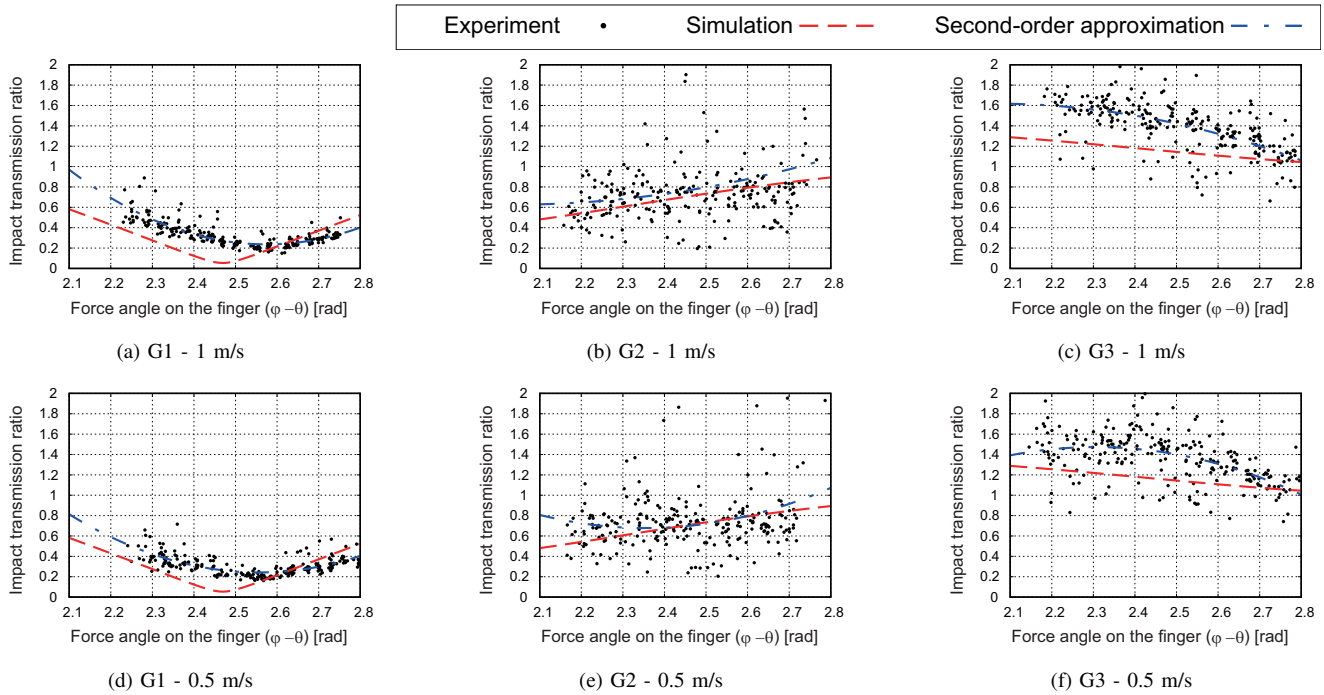

(a) G1 - 1 m/s (b) G2 - 1 m/s (c) G3 - 1 m/s

(d) G1 - 0.5 m/s (e) G2 - 0.5 m/s (f) G3 - 0.5 m/s

Fig. 8: Impact transmission ratio calculated from the experiment

transmission ratio reaches its minimum in the experimental results for G1, the ratio is approximately 0.2 for G1, whereas it is around 0.7 and 1.4 for G2 and G3, respectively. This result demonstrates the high impact attenuation capability of G1 and validates the proposed design strategy.

V. CONCLUSIONS

In this paper, we proposed a design strategy based on the CoP theory as a method to mitigate impact force applied to the gripper's shaft during high-speed contact. This is assumed as an application to grippers using direct drive or quasi-direct drive mechanisms. Additionally, collision experiments using a single finger demonstrated the validity of the theory and the effectiveness of the design.

However, the dynamic model presented in this paper does not consider the effect of the actuator friction. Although the effects of the arm acceleration and gravity were neglected, this assumption was reasonably justified. Thus, the validity of the proposed design strategy is currently limited to direct-drive actuators with minimal viscous resistance. Future work should examine the friction effects and validate the approach with quasi-direct-drive systems (low-reduction-ratio geared motors).

In addition, the finger geometry in this study was determined through iterative adjustments in CAD, which is inefficient and impractical. To address this limitation, it is necessary to develop a generative design framework that integrates the derived design conditions into an optimization process.

REFERENCES

[1] A. Bhatia, A. M. Johnson, and M. T. Mason, Direct Drive Hands: Force-Motion Transparency in Gripper Design, in *Proc. Robotics: Science and Systems (RSS)*, Freiburg im Breisgau, Germany, June 22-26, 2019.

[2] K. H. Mak, P. Xu, and J. Seo, High-Speed Scooping: An Implementation through Stiffness Control and Direct-Drive Actuation, in *Proc. IEEE Int. Conf. Robotics and Automation (ICRA)*, London, United Kingdom, 2023, pp. 10261-10267.

[3] F. Ostyn, B. Vanderborght, and G. Crevecoeur, Design and Control of a Quasi-Direct Drive Robotic Gripper for Collision Tolerant Picking At High Speed, *IEEE Robot. Autom. Lett.*, vol. 7, no. 3, pp. 7692-7699, July 2022.

[4] M. Guo et al., Blue Gripper: A Robust, Low-Cost, and Force-Controlled Robot Hand, in *Proc. IEEE Int. Conf. Automation Science and Engineering (CASE)*, Vancouver, BC, Canada, 2019, pp. 1505-1510.

[5] S. Tanaka, K. Koyama, T. Senoo, M. Shimojo, and M. Ishikawa, High-speed Hitting Grasping with Magripper, a Highly Backdrivable Gripper using Magnetic Gear and Plastic Deformation Control, in *Proc. IEEE/RSJ Int. Conf. Intelligent Robots and Systems (IROS)*, Las Vegas, NV, USA, 2020, pp. 9137-9143.

[6] Y. Shimizu, A. Kakogawa, and S. Kawamura, A two-fingered independent gripper capable of high-speed contact grasping using low-friction geared electric motors, in *Proc. 2025 IEEE Int. Conf. Real-time Comput. Robot. (RCAR)*, Toyama, Japan, 2025, pp. 305–310.

[7] T. Irie and H. Yamada, *Fundamentals of Mechanical Engineering: Industrial Mechanics*, 2nd ed. Tokyo, Japan: Ohmsha, 2018. [in Japanese]

[8] S. Hirose, *Robot Engineering*, Revised ed. Tokyo, Japan: Shokabo, 2005. [in Japanese]

[9] I. S. Paraskevas and E. Papadopoulos, On the use of the center of percussion for space manipulators during impacts, in *Proc. IEEE Int. Conf. Robotics and Automation (ICRA)*, Karlsruhe, Germany, 2013.

[10] I. S. Paraskevas and E. Papadopoulos, Parametric sensitivity and control of on-orbit manipulators during impacts using the Centre of Percussion concept, *Control Eng. Pract.*, 2015.

[11] H. Arisumi, J.-R. Chardonnet, A. Kheddar, and K. Yokoi, Dynamic Lifting Motion of Humanoid Robots, in *Proc. IEEE Int. Conf. Robotics and Automation (ICRA)*, Rome, Italy, 2007.

[12] K. Ioi, T. Kawabuchi, A. Suda, and K. Moriya, Mechanical and control design of caster for low vibrations and crashes of carts, in *Proc. IEEE Int. Conf. Mechatronics and Automation (ICMA)*, Beijing, China, 2011.